11-1-2018

Anti-apoptotic effects of human placental hydrolysate against hepatocyte toxicity in vivo and in vitro

Dong Ho Bak
Chung-Ang University, College of Medicine

Jungtae Na
Chung-Ang University, College of Medicine

Mi Ji Choi
Chung-Ang University, College of Medicine

Byung Chul Lee
Chung-Ang University, College of Medicine

Chang Taek Oh
Green Cross WellBeing Corporation

See next page for additional authors

Recommended Citation

Bak, D.-H., Na, J., Choi, M. J., Lee, B. C., Oh, C. T., Kim, J.-Y., Han, H. J., Kim, M. J., Kim, T. H., & Kim, B. J. (2018). Anti-apoptotic effects of human placental hydrolysate against hepatocyte toxicity in vivo and in vitro. International Journal of Molecular Medicine, 42(5), 2569–2583. https://doi.org/10.3892/ijmm.2018.3830

Authors

Dong Ho Bak, Jungtae Na, Mi Ji Choi, Byung Chul Lee, Chang Taek Oh, Jeom Yong Kim, Hae Jung Han, Moo Joong Kim, Tae Ho Kim, and Beom Joon Kim

Anti-apoptotic effects of human placental hydrolysate against hepatocyte toxicity *in vivo* and *in vitro*

DONG-HO BAK[1,2*], JUNGTAE NA[1*], MI JI CHOI[1,2*], BYUNG CHUL LEE[1], CHANG TAEK OH[3], JEOM-YONG KIM[3], HAE JUNG HAN[3,4], MOO JOONG KIM[5], TAE HO KIM[6] and BEOM JOON KIM[1,2]

[1]Department of Dermatology, College of Medicine; [2]Department of Medicine, Graduate School, Chung-Ang University, Seoul 06973; [3]Research and Development Center, Green Cross WellBeing Corporation, Seongnam, Gyeonggi 13595; [4]Department of Microbiology and Medical Research Institute, Chungbuk National University, College of Medicine, Cheongju, Chungcheongbuk 28644, Republic of Korea; [5]Fort Hays State University, Hays, KS 67601, USA; [6]Division of Gastroenterology, Department of Internal Medicine, Bucheon St. Mary's Hospital, The Catholic University of Korea, Bucheon-si, Gyeonggi 14647, Republic of Korea

Abstract. Apoptosis and oxidative stress are essential for the pathogenesis of acute liver failure and fulminant hepatic failure. Human placental hydrolysate (hPH) has been reported to possess antioxidant and anti-inflammatory properties. In the present study, the protective effects of hPH against D-galactosamine (D-GalN)- and lipopolysaccharide (LPS)-induced hepatocyte apoptosis were investigated *in vivo*. In addition, the molecular mechanisms underlying the anti-apoptotic activities of hPH against D-GalN-induced cell death *in vitro* were examined. Male Sprague-Dawley rats were injected with D-GaIN/LPS with or without the administration of hPH. Rats were sacrified 24 h after D-GaIN/LPS intraperitoneal injection, and the blood and liver samples were collected for future inflammation and hepatotoxicity analyses. Changes in cell viability, apoptosis protein expression, mitochondrial mass, mitochondrial membrane potential, reactive oxygen species generation, and the levels of proteins and mRNA associated with a protective mechanism were determined in HepG2 cells pretreated with hPH for 2 h prior to D-GalN exposure. The findings suggested that hPH treatment effectively protected against D-GalN/LPS-induced hepatocyte apoptosis by reducing the levels of alanine aminotransferase, aspartate aminotransferase, lactate dehydrogenase, interleukin-6, and tumor necrosis factor-α, and increasing the level of proliferating cell nuclear antigen. It was also found that hPH inhibited the apoptotic cell death induced by D-GalN. hPH activated the expression of antioxidant enzymes, including superoxide dismutase, glutathione peroxidase, and catalase, which were further upregulated by the Kelch-like ECH2-associated protein 1-p62-nuclear factor-erythroid 2-related factor 2 pathway, a component of oxidative stress defense mechanisms. Furthermore, hPH markedly reduced cytosolic and mitochondrial reactive oxygen species and rescued mitochondrial loss and dysfunction through the reduction of damage-regulated autophagy modulator, p53, and C/EBP homologous protein. Collectively, hPH exhibited a protective role in hepatocyte apoptosis by inhibiting oxidative stress and maintaining cell homeostasis. The underlying mechanisms may be associated with the inhibition of endoplasmic reticulum stress and minimization of the autophagy progress.

Correspondence to: Dr Tae Ho Kim, Division of Gastroenterology, Department of Internal Medicine, Bucheon St. Mary's Hospital, The Catholic University of Korea, 327 Sosa-ro, Wonmi-gu, Bucheon-si, Gyeonggi 14647, Republic of Korea
E-mail: kimtaeho@catholic.ac.kr

Dr Beom Joon Kim, Department of Dermatology, College of Medicine, Chung-Ang University Hospital, 102 Heukseok-ro, Dongjak-gu, Seoul 06973, Republic of Korea
E-mail: beomjoon74@gmail.com

*Contributed equally

Introduction

Acute liver failure (ALF), sometimes referred to as fulminant hepatic failure, is a severe liver disease characterized by coagulopathy and liver inflammation in patients with previously normal liver function (1). The onset of liver injury, often accompanied by endotoxemia and hepatocyte death, can result in high mortality rates in animals and humans, due to the lack of an effective therapy for ALF, other than liver transplantation (2).

The administration of D-galactosamine (D-GalN) and lipopolysaccharides (LPS) establishes an animal model for ALF; it severely impairs liver function in laboratory animals, and can be used to investigate ALF (3). LPS, a type of endotoxin, can cause liver tissue damage through activation of inflammatory cytokines, including interleukin (IL)-1β, IL-6,

tumor necrosis factor (TNF)-α, and interferon-γ (4). A report suggests that LPS as an inflammatory mediator can stimulate the production of reactive oxygen species (ROS) and can be used broadly to induce research models of ALF (5). A D-GalN/LPS-induced animal model of ALF is representative of human liver failure and has been widely used to investigate mechanisms and potential therapeutic drugs for clinical use in treating ALF (2). Increasing evidence has shown that oxidative stress and hepatocyte apoptosis are two important pathogenic factors that contribute to D-GalN/LPS-induced ALF (6,7).

The evaluation of mechanisms involved in D-GalN/LPS-induced hepatic apoptosis has indicated that mitochondria are critical targets for drug toxicity through the formation of reactive metabolites (8,9). In response to oxidative stress, the cellular machinery of the antioxidative response is mediated by cytoprotective enzymes in the liver. When it to comes to oxidation, nuclear factor-E2-related factor 2 (Nrf2), a key sensor in antioxidative stress systems, regulates cellular defense against oxidative damage (10), contributing to diverse cellular functions, including proliferation, inflammation and lipid synthesis (11). The aberrant expression or function of Nrf2 has been linked to pathologies, including hepatic steatosis (12) and diabetic nephropathy (13). Although Nrf2 is regularly sequestered by Kelch-like ECH2-associated protein 1 (Keap1) in the cytoplasm (14), when activated, it translocates into the nucleus and upregulates antioxidant response element (ARE) genes, including superoxide dismutase (SOD)1/SOD2, catalase, glutamate-cysteine ligase catalytic subunit (GCLC), glutamate-cysteine ligase regulatory subunit (GCLM), heme oxygenase-1 (HO-1), cytochrome P450s, multidrug-resistant proteins and NAD(P)H dehydrogenase quinone 1 (NQO1) (15,16).

In general, the autophagy-dependent degradation of impaired organelles, including the selective degradation of the endoplasmic reticulum (ER; reticulophagy), mitochondria (mitophagy), and lipid droplets (lipophagy), is a crucial cellular pathway for maintaining cell homeostasis (17,18). However, autophagy is also regarded as a pro-apoptotic factor and causes 'type II' programmed cell death (19). The cellular damage mediated by p53 has a pathological role in the progression of hepatosteatosis. It is noteworthy that p53 can promote the expression of damage-regulated autophagy modulator (DRAM), an inducer of autophagy-mediated apoptosis (20).

Previous studies have revealed that human placental hydrolysate (hPH) is a rich source of various bioactive substances, including polydeoxyribonucleotides, RNA, DNA, peptides, amino acids, enzymes, and trace elements, among others (21). Human placenta has been demonstrated to possess various therapeutic properties ranging from wound healing to immunomodulation (22). The use of aqueous extract of human placenta in wound healing, ophthalmology, infertility, apoplexy, and epilepsy has evolved from folk knowledge to modern scientific practice (23). In a previous clinical trial, it was identified that treatment of hPH ameliorated alcoholic or nonalcoholic steatohepatitis in patients (24,25). In addition, hPH has been shown to have a protective effect in ALF via an anti-inflammatory response (26). However, the mechanism underlying this anti-apoptotic action and the defense mechanism remain to be fully elucidated. Given the various uses of human placenta for intervention in different diseases, the present study was undertaken to investigate the protective effects of hPH against apoptotic hepatocyte cell death *in vivo* and *in vitro*.

Materials and methods

Reagents and antibodies. All chemicals and solvents used were of the highest analytical grade available. Cell culture supplies and media, including fetal bovine serum (FBS), phosphate-buffered saline (PBS), and penicillin-streptomycin were purchased from Thermo Fisher Scientific, Inc. (Waltham, MA, USA). The Cell Counting Kit-8 (CCK-8; cat. no. CK04-11) was from Dojindo Molecular Laboratories, Inc. (Kumamoto, Japan). Protease inhibitor cocktail (cat. no. P8340) and D-GalN (cat. no. G0500) were purchased from Sigma-Aldrich; EMD Millipore (Billerica, MA, USA). Anti-proliferating cell nuclear antigen (PCNA; cat. no. ab15497), anti-Tomm20 (cat. no. ab56783) and anti-Lamin B1 (cat. no. ab16048) antibodies were purchased from Abcam (Cambridge, UK). Anti-poly (ADP) ribose polymerase (PARP; cat. no. 9532S) antibody was purchased from Cell Signaling Technology, Inc. (Beverly, MA, USA). Anti-B-cell lymphoma 2 (BCL2; cat. no. SC-7382), anti-Bcl-2-associated X protein (BAX; cat. no. SC-526), anti-DRAM (cat. no. SC-81713), anti-SOD1 (cat. no. SC-17767), anti-SOD2 (cat. no. SC-130345), anti-glutathione peroxidase (GPx; cat. no. SC-133160), anti-Catalase (cat. no. SC-271358), anti-Keap1 (cat. no. SC-365626), anti-HO-1 (cat. no. SC-136960), anti-p53 (cat. no. SC-126), anti-GAPDH (cat. no. SC-20357), and anti-Nrf2 (cat. no. SC-81342) antibodies were purchased from Santa Cruz Biotechnology, Inc. (Santa Cruz, CA, USA). Anti-microtubule-associated protein 1A/1B-light chain 3 (LC3)I/II (cat. no. PM036), anti-phosphorlyated-p62 (cat. no. PM074), and anti-p62 (cat. no. PM045) antibodies were purchased from MBL International Corporation (Woburn, MA, USA). hPH (Laennec inj.) was manufactured by Green Cross WellBeing Corporation (Seongnam, Korea) through the hydrolysis of human placenta with HCl and pepsin.

Animals and experimental design. Sprague-Dawley rats (SD) rats (male, 6-8 weeks old, weighing ~200-250 g each) were purchased from Raonbio, Inc. (Yongin, Korea). These rats were provided with adequate food and water *ad libitum* and were housed in clean cages for 1 week. The laboratory temperature was 24±1°C and relative humidity was 40-80%. All animal experiments were performed according to the Guide for the Care and Use of Laboratory Animals as published by the US National Institutes of Health. The present study was reviewed and approved by the Animal Welfare and Research Ethics Committee at Chung-Ang University (Seoul, Korea; 2017-00003). Acute liver injury was induced by intraperitoneal injection of LPS (15 µg/kg) together with D-GalN (700 mg/kg) dissolved in normal saline, which can increase the sensitivity of hepatocytes. Blood was collected from the inferior vena cava 24 h following injection of D-GalN/LPS. The SD rats were then dissected, and liver tissues were removed immediately for histological detection. Normal PBS was used in control rats. hPH (1.2, 2.4, and 3.6 ml/kg) was injected subcutaneously into each mouse 24, 48, and 72 h prior to D-GalN/LPS injection. As a negative control, only D-GalN/LPS was injected.

Evaluation of serum alanine aminotransferase (ALT) and aspartate aminotransferase (AST). The collected blood samples were stored overnight at 4°C. The serum was isolated the subsequent day following centrifugation at 15,928 x g for 10 min at 4°C. The ALT and AST were detected using a Hitachi 7600 Series automatic biochemical analyzer (Hitachi, Ltd., Tokyo, Japan).

Enzyme-linked immunosorbent assay (ELISA) of cytokines. Based on a previous study, blood was collected for measuring TNF-α (cat. no. 438207) and IL-6 (cat. no. 437107) at 24 h post-D-GalN/LPS injection. The serum was separated by centrifugation at 15,928 x g at 4°C for 10 min. The cytokines were measured using mouse ELISA kits (BioLegend, Inc., San Diego, CA, USA) according to the manufacturer's protocol.

Histopathological evaluation. The liver tissues were immersed in normal 10% neutral buffered formalin and fixed for 48 h, dehydrated in a series of graded ethanol, embedded in paraffin wax, and cut into 5-μm sections. The paraffin-embedded sections were stained with hematoxylin and eosin (H&E) for pathological analysis under a light microscope. Histological changes were evaluated using a point-counting method for the severity of hepatic injury using an ordinal scale, as previously described (27). Briefly, the H&E-stained sections were evaluated at x400 magnification using the point-counting method for the severity of hepatic injury with an ordinal scale as follows: grade 0, minimal or no evidence of injury; grade 1, mild injury consisting of cytoplasmic vacuolation and focal nuclear pyknosis; grade 2, moderate to severe injury with extensive nuclear pyknosis, cytoplasmic hypereosinophilia, and loss of intercellular borders; and grade 3, severe necrosis with disintegration of hepatic cords, hemorrhage, and neutrophil infiltration.

Measurement of apoptosis via TUNEL assay. TUNEL was performed to analyze DNA fragmentation indicative of cellular apoptosis using the *in situ* cell death detection kit (cat. no. ab206386, Abcam), according to the manufacturer's protocol. The paraffin wax-embedded tissue sections were treated with proteinase K, and endogenous peroxidase activity was blocked with hydrogen peroxide. The sections were incubated at 37°C with the terminal TdT nucleotide mixture for 1 h. The reactions were then terminated, and the slides were rinsed with PBS. Nuclear labeling was developed with horseradish peroxidase and diaminobenzidine. The number of apoptotic cells in each slide from at least five different fields was analyzed using Image-Pro Plus software (version 6.0 for Windows; Media Cybernetics, Inc., Rockville, MD, USA) with the assistance of a microscope (DM750; Leica Microsystems GmbH, Wetzlar, Germany). The number of positive cells was averaged for statistical analysis.

Liver immunohistochemistry. The paraffin sections were de-paraffinized and rehydrated. Endogenous peroxidase was inactivated by incubation in 0.3% hydrogen peroxide in absolute methanol for 30 min. The sections were incubated in 5% skim milk for 30 min at room temperature. Antigen retrieval was performed by microwave (700 W) treatment in 10 mM citrate buffer (pH 6.0) for 15 min. The sections were incubated overnight at 4°C with anti-PCNA primary antibody (Abcam) at a dilution of 1:500. Following washing with PBS, the sections were incubated at room temperature for 30 min in secondary antibody (Goat Anti-Rabbit; cat. no. ab205718; Abcam; 1:1,000). A brown color was developed with 3 diaminobenzidine for 2-4 min, and the sections were then washed in distilled water. The number of positively stained brown nuclei (denoting PCNA) in each slide from at least five different fields was analyzed using Image-Pro Plus software (version 6.0 for Windows) with the assistance of a microscope (DM750, Leica Microsystems GmbH). The number of positive cells was averaged for statistical analysis.

Cell culture and treatment. Human HepG2 cells, the HepG2 (ATCC HB 8065) cells were purchased from the Korea Cell Line Bank (Seoul, Korea), and were cultured in Dulbecco's modified Eagle's medium (DMEM) with 10% (v/v) heat-inactivated FBS and 1% penicillin and incubated in a humidified incubator with 5% CO_2, 95% air at 37°C. A dose of 5% hPH was used in the time-course investigation of the induction of antioxidant enzymes by hPH. To investigate the protective effects of hPH and its active mechanism on HepG2 cells challenged by D-GaIN (Sigma; EMD Millipore), the cells were pretreated with hPH for 2 h, stimulated with 50 mM D-GaIN at 37°C, and harvested for the indicated experiments.

Cell viability assay. The HepG2 cells, treated as described above, were further treated with 50 mM D-GalN and incubated for another 24 h, following which the cell viability was determined using CCK-8 (Dojindo Molecular Technologies, Inc.). To determine cell viability, the HepG2 cells were seeded in 96-well plates at a density of $1x10^4$ cells/ml and grown for 24 h in a 37°C incubator. When the cells attained 70-80% confluence, they were either left untreated (control group) or treated with D-GalN (50 mM), 5% hPH, or 5% hPH + D-GalN (50 mM). Following incubation for 24 h, cell morphology changes were observed under Olympus inverted microscopes (Olympus Corporation, Tokyo, Japan). The supernatants were discarded, following which 10% CCK-8 solution in fresh DMEM (100 μl) were added to each well. The cells were then incubated at 37°C for 1 h, and the absorbance was measured at 450 nm directly in the wells using a SpectraMax i3x Multi-Mode detection platform (Molecular Devices LLC, Sunnyvale, CA, USA).

Measurement of LDH release. The LDH in the culture medium was assessed with 0.2 mM NADH and 0.4 mM pyruvic acid in up to 200 μl PBS at pH 7.4. The LDH concentration in the sample was proportional to the rate of NADH oxidation measured by absorbance at 334 nm (OD/min) using the SpectraMax i3x Multi-Mode detection platform. The LDH concentration in the culture media was calculated using a commercial standard LDH assay kit purchased from Abnova (cat. no. KA0785, Taipei, Taiwan).

DAPI staining. Morphological changes in the apoptotic cells were assessed by fluorescent microscopy following DAPI staining. Briefly, the HepG2 cells were seeded at a density of $1x10^5$ cells/ml in 6-well plates and grown for 24 h in a 37°C incubator. Following washing once with PBS, the cells were

either left untreated (control group) or treated with D-GalN (50 mM), 5% hPH, or 5% hPH + D-GalN (50 mM). Following incubation for 24 h, the cells were fixed in 4% formaldehyde for 1 h, and permeabilized with 0.1% Triton X-100 (Biosesang, Inc., Seongnam, Korea) for 5 min. Subsequently, DNA-specific fluorochrome DAPI (Invitrogen; Thermo Fisher Scientific, Inc.) was applied to each well, following which samples were incubated for 10 min in the dark at room temperature. Finally, the cells were washed three times with PBS and examined using a confocal microscope (Carl Zeiss AG, Oberkochen, Germany).

Annexin V-fluorescein isothiocyanate (FITC)/propidium iodide (PI) staining and fluorescence images. For apoptotic cell analysis, the HepG2 (1x10^4/well) cultures in 96-well black plates were exposed to the indicated treatments for 12 h. The assay was performed according to the manufacturer's protocol (BD Biosciences, San Jose, CA, USA). Briefly, the cells were washed twice with PBS and again with binding buffer. Annexin V-fluorescein isothiocyanate and PI were added to each sample, and the mixture was incubated at room temperature for 15 min. The absorbance was read directly in the wells at 494/518 nm for FITC Annexin V and 535/617 nm for PI using the SpectraMax i3x Multi-Mode detection platform. The populations staining positive for Annexin V and PI were compared with the untreated group.

The HepG2 cells were grown to ~70% confluence; 1x10^5 cells were collected in a Petri dish and either left untreated (control group) or treated with D-GalN (50 mM), 5% hPH, or 5% hPH + D-GalN (50 mM); and then incubated for 24 h. The cells were then washed with PBS and stained with 10 μg/ml PI for 5 min, and fluorescent images were observed under a DP70 fluorescence microscope with DP Controller software (Olympus Corporation; ver. 3.2.276.2).

Measurement of ROS. Cytosolic and mitochondrial ROS were measured on a 96-well plate reader as previously described (28). Briefly, the HepG2 cells were seeded at a concentration of 1x10^4 cells per well in black 96-well flat bottom plates (Thermo Fisher Scientific, Inc.) and allowed to adhere overnight. Following seeding, the cells were washed and incubated with serum-starved medium, D-GalN (50 nM), 5% hPH, or 5% hPH + D-GalN (50 mM) for 4 h, followed by incubation with 2',7'-dichlorofluorescin diacetate (DCFH-DA; 10 μM, ex/em: 518/605 nm; Invitrogen; Thermo Fisher Scientific, Inc.) or MitoSOX™ (5 μM, ex/em: 510/580 nm; Invitrogen; Thermo Fisher Scientific, Inc.) for 20 min. The oxidative products were measured with the SpectraMax i3x Multi-Mode detection platform.

Measurement of mitochondrial membrane potential ($\Delta\Psi m$). The $\Delta\Psi m$ of intact cells was measured as previously described, (29) with modifications. Briefly, the cells were washed with PBS and TMRE (200 nM, ex/em: 549/582 nm; Invitrogen; Thermo Fisher Scientific, Inc.) was added to the cell suspension. The cells were incubated at 37˚C for 30 min in the dark. The $\Delta\Psi m$ was measured using the SpectraMax i3x Multi-Mode detection platform. The percentage and mean fluorescence intensity level of the mass were calculated for each sample.

Determination of mitochondrial mass. Mitochondrial mass was measured according to fluorescence levels following staining with MitoTracker Green FM (100 nM, ex/em: 490/525 nm; Invitrogen; Thermo Fisher Scientific, Inc.) at 37˚C for 30 min. Subsequently, the cells were washed once in PBS and promptly evaluated using the SpectraMax i3x Multi-Mode detection platform. The percentage and mean fluorescence intensity level of the mass were calculated for each sample.

Fluorescence microscopy. The cells (1x10^6 cells/well) were prepared on sterilized glass coverslips (BD Biosciences) in triplicate and then fixed in 4% paraformaldehyde in PBS for 10 min, permeabilized with 0.25% Triton X-100 in PBS for 10 min and incubated with primary antibodies against Tomm20 (Abcam; 1:500), Nrf2 (Santa Cruz Biotechnology, Inc.; 1:500), and LC3 (Abcam; 1:500) for 12 h at 4˚C incubator. The cells were washed to remove excess primary antibodies and incubated with the appropriate fluorescently labeled secondary antibodies (1:1,000) for 1 h at room temperature. Following mounting of slides, fluorescence images were acquired using a confocal microscope (LSM700, Carl Zeiss AG).

Western blot analysis. The cells were lysed in cell lysis buffer [62.5 mM Tris-HCl (pH 6.8), 2% sodium dodecyl sulfate (SDS), 5% β-mercaptoethanol, 2 mM phenylmethylsulfonyl fluoride, protease inhibitors (Complete™; Roche Diagnostics GmbH, Mannheim, Germany), 1 mM Na$_3$VO$_4$, 50 mM NaF and 10 mM EDTA]. The protein content of the lysates was determined using BCA Protein Assay reagent (cat. no. 23225; Pierce; Thermo Fisher Scientific, Inc.). A 20 μg sample of protein per lane was separated by 12% SDS-polyacrylamide gel electrophoresis and blotted onto polyvinylidene fluoride membranes (EMD Millipore) which were then saturated with 5% powdered milk in Tris-buffered saline containing 0.5% Tween-20. The blots were then incubated with the appropriate primary antibodies at a dilution of 1:1,000 or 1:2,000 for 12 h in a 4˚C incubator, and further incubated with horseradish peroxidase-conjugated secondary antibody (1:10,000) for 2 h at 37˚C. The bound antibodies were detected using enhanced chemiluminescence (Amersham; GE Healthcare Life Sciences, Chalfont, UK). Images of the blotted membranes were captured using the LAS-1000 lumino-image analyzer (Fujifilm, Tokyo, Japan). The protein levels were compared to those of the appropriate loading control (GAPDH or non-phosphorylated proteins).

Reverse transcription-quantitative polymerase chain reaction (RT-qPCR) analysis. Total RNA was extracted from the dorsal skin using TRIzol (Invitrogen; Thermo Fisher Scientific, Inc.). First-strand cDNA synthesis from the total RNA template was performed with PrimeScript RT master mix (Takara Bio, Inc., Tokyo, Japan). The resulting cDNA was subjected to real-time PCR (complementary cDNA, 2 μl; primer, 3 μl; 2X premix SYBR, 5 μl), using qPCR 2X PreMIX SYBR (Enzynomics, Seoul, Korea) and a CFX-96 thermocycler (Bio-Rad Laboratories, Inc., Hercules, CA, USA). The PCR conditions used to amplify all genes were as follows: 10 min at 95˚C and 40 cycles of 95˚C for 10 sec, 60˚C for 15 sec, and 72˚C for 20 sec. The expression data were calculated from the quantification cycle (Cq) value using the ΔCq method of

quantification (30). GAPDH was used for normalization. The oligonucleotides that were used for qPCR were as follows: Human ATG8, forward 5'-CGCACCTTCGAACAAAGA GT-3' and reverse, 5'-GACCATGCTGTGTCCGTT C-3'; human beclin 1 (BECN1), forward 5'-AACCTCAGCCGA AGACTG AA-3' and reverse, 5'-CCTCTAGTGCCAGCTCCT TT-3'; human cathepsin D (CTSD), forward 5'-CAAGTTCGA TGGCATCCTGG-3' and reverse 5'-CGGGTGACATTCAGG TAGGA-3'; human lysosomal-associated membrane protein 1 (LAMP1), forward 5'-CTTTCAAGGTGGAAGGTGzGC-3' and reverse 5'-GATAGTCTGGTAGCCTGCGT-3'; human activating transcription factor (ATF)6, forward 5'-GTGTCA GAGAACCAGAGGCT-3' and reverse 5'-GGTGCCTCCTTT GATTTGCA-3'; human ATF4, forward 5'-ACACTGCTTACG TTGCCATG-3' and reverse 5'-AGACCCACAGAGAACACC TG-3'; human C/EBP homologous protein (CHOP), forward 5'-CATTGCCTTTCTCCTTCGGGG-3' and reverse 5'-CCA GAGAAGCAGGGTCAAGA-3'.

Statistical analysis. All quantitative data are presented as the mean ± standard error of the mean for three independent experiments. Statistical analyses were performed using the statistical package for SPSS software version 17.0 (IBM Corp., Armonk, NY, USA). Differences between two groups were evaluated using a paired Student's t-test. For multiple comparisons, one-way analysis of variance was used followed by Tukey's multiple comparisons test. $P<0.05$ was considered to indicate a statistically significant difference.

Results

Effects of hPH on mortality rates of D-GalN/LPS-treated rats. Acute liver injury leads to high mortality rates in rats. Therefore, the present study assessed the effects of hPH on D-GalN (700 mg/gg)/LPS (15 µg/kg)-induced mortality. To investigate whether hPH can protect against liver injury in rats due to D-GalN/LPS, the survival rate of D-GalN/LPS + hPH-treated rats was monitored for 24 h (n=12). All saline-injected rats survived as the normal control group (n=12). No significant differences in gross liver examination, body weight, or liver weight were found between groups (Fig. 1A-C). As shown in Fig. 1D, a number of rats died 7 h following D-GalN/LPS injection, and the survival rate was 33.3% at 24 h. However, it was found that hPH pretreatment effectively increased the survival rate of rats with liver injury induced by D-GalN/LPS. Pretreatment with hPH (1.2 ml/kg) increased the survival rate to 83.3%, and all hPH (2.4 and 3.6 ml/kg)-treated rats survived. These results suggested that pretreatment with hPH effectively protected against D-GalN/LPS-induced mortality.

Effects of hPH on serum levels of ALT, AST, and inflammatory cytokines in LPS/GalN-induced liver failure in rats. The serum levels of AST, ALT, LDH, and inflammatory cytokines are well-established markers of hepatic injury (31). In order to investigate the effects of hPH on D-GalN/LPS-induced liver damage, hematological tests were performed. Serum (n=4-6) was collected to detect AST, ALT, LDH, IL-6, and TNF-α. As shown in Fig. 1E-G, LPS/D-GalN markedly increased serum levels of AST, ALT, and LDH, whereas hPH reduced these elevations. As hepatocyte injury resulting from acute liver

injury is accompanied by an elevation in inflammatory cytokines (32), the present study examined the effect of hPH on hepatotoxicity by measuring serum levels of IL-6 and TNF-α (Fig. 1H and I). The D-GalN/LPS-treated rats exhibited significant increases in levels of IL-6 and TNF-α compared with normal rats. In addition, hPH pretreatment significantly inhibited the release of these pro-inflammatory cytokines compared with the LPS/D-GalN group. These results suggested that hPH effectively protected against LPS/D-GalN-induced liver degeneration and inflammatory responses.

Effects of hPH on hepatotoxicity of hepatocytes. The present study also investigated histological changes following liver injury to confirm the protective effects of hPH. The rats treated with D-GalN/LPS showed severe histopathological degeneration evidenced by severe intrahepatic hemorrhaging, apoptosis, necrosis, ballooned hepatocytes, and hepatocytes expanded by fat vacuoles, whereas hPH (1.2, 2.4 and 3.6 ml/kg) treatment ameliorated these changes (Fig. 2A). It has been suggested that D-galN/LPS-induced imbalance between apoptosis and proliferation in hepatocytes is responsible for the impairment of liver function. Therefore, hPH-mediated modulations of proliferation (PCNA) and apoptosis (TUNEL) were also evaluated by immunohistochemical analysis (Fig. 2B and C). A high expression of PCNA and low numbers of TUNEL-positive cells were observed in the control group. However, D-GalN/LPS markedly reduced PCNA immunoreactivity and significantly increased the number of apoptotic cells. By contrast, pre-administration of hPH resulted in an increase of PCNA-positive cells and reduced the number of apoptotic cells in all three dose groups. Graphs showing results of the staining experiments are shown in Fig. 2D-F. These observations indicated that hPH pretreatment ameliorated hepatic injury by reducing D-GalN/LPS-induced hepatocyte damage in rats.

hPH protects hepatocytes against D-GalN-induced apoptosis. Hepatocyte apoptosis is important in the pathogenesis of liver disease, including ALF (33). D-GalN induces hepatocyte cell death *in vivo* (34) and *in vitro* (35); it offers a suitable experimental model based on its capacity to reduce the intracellular pool of uridine monophosphate in hepatocytes, inhibiting the synthesis of RNA and proteins, and leading to cell apoptosis. Therefore, the present study investigated whether D-GalN-induced hepatotoxicity occurred in HepG2 cells. Following D-GalN stimulation, cell viability decreased markedly in a dose-dependent manner. The results revealed a reduction of 50% at 50 mM D-GalN and of 82% at 100 mM D-GalN in the HepG2 cells (Fig. 3A). The cytotoxic effects of hPH on HepG2 cells have not been examined previously. The present study used a CCK-8 assay to evaluate the dose-dependent cytotoxic effects of hPH on HepG2 cells. The results showed that stimulation with hPH had no significant effect on cell viability at various concentrations (1.25-5% in serum-free DMEM) over 24 h. Therefore, hPH was used at a concentration of 5% in subsequent experiments (Fig. 3B). In addition to the D-GalN-induced decrease in cell viability being attenuated by pretreatment with hPH, the concentration of LDH released from the hepatocytes was also reduced in the D-GalN + 5% hPH-stimulated cells, compared with the
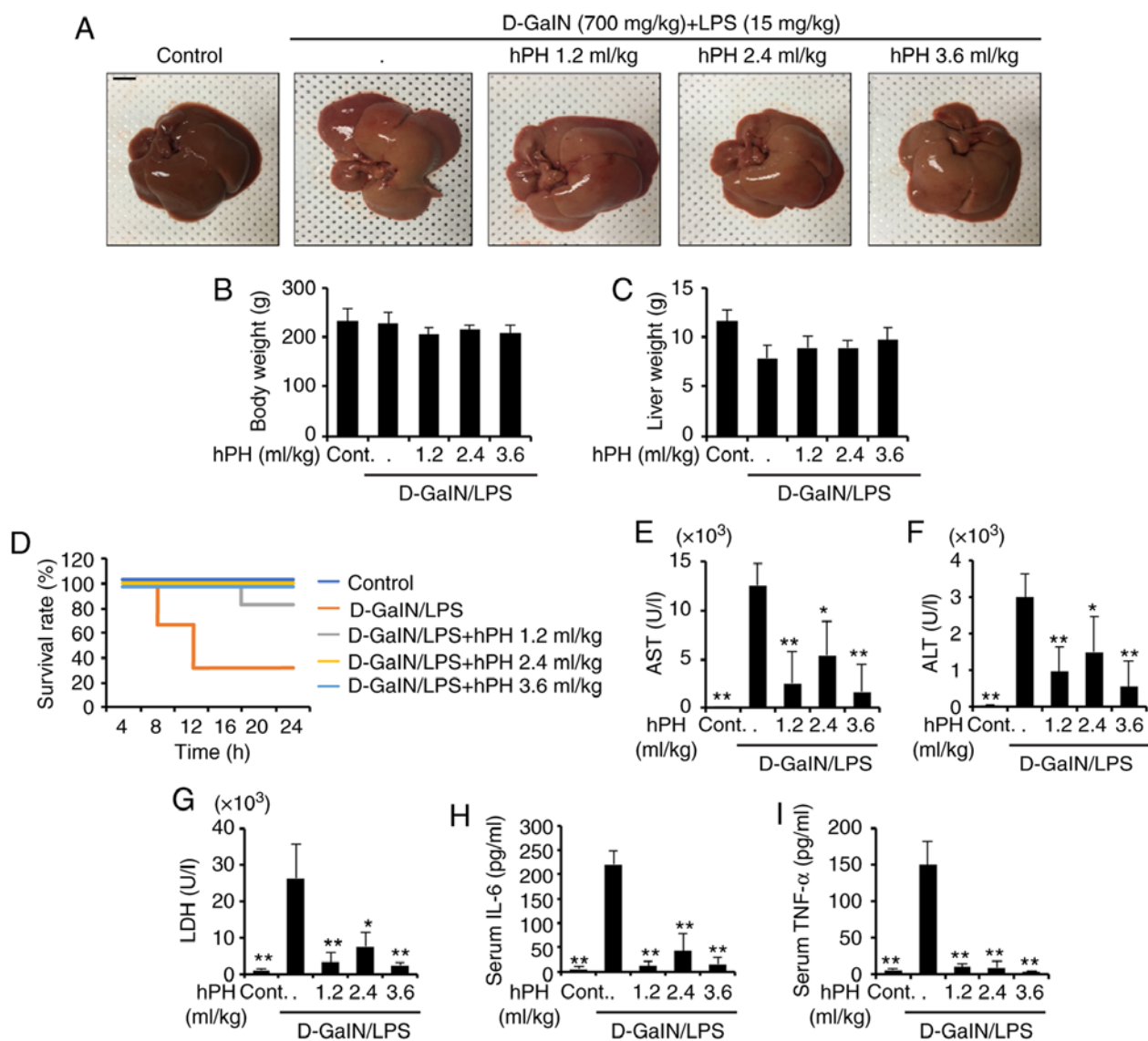
Figure 1. Protective effects of hPH treatment on D-GalN/LPS-induced acute liver failure. hPH (1.2, 2.4, or 3.6 ml/kg) was subcutaneously administered to rats three times at intervals of 24 h, followed by exposure to 700 mg/kg D-GalN and 15 µg/kg LPS (D-GalN/LPS). Livers from each experimental group were examined 24 h following D-GalN/LPS challenge. (A) Gross image of livers. Scale bar=1 cm (B) Animal weights (n=4-6) were measured just prior to sacrifice; with no statistical difference among groups. (C) Liver weights were measured following sacrifice, with no statistical difference among groups (n=4-6). (D) Survival rates of rats were observed for 24 h following D-GalN/LPS exposure (n=12). Serum (n=4-6) was collected from animals 24 h following exposure to D-GalN/LPS to determine levels of (E) AST, (F) ALT, (G) LDH, (H) IL-6, and (I) TNF-α. All data are presented as the mean ± standard error of the mean. *P<0.05 and **P<0.01, vs. D-GalN/LPS group. hPH, human placental hydrolysate; D-GalN, D-galactosamine; LPS, lipopolysaccharide; Cont, control; AST, aspartate aminotransferase; ALT, alanine aminotransferase; LDH, lactate dehydrogenase; IL-6, interleukin-6; TNF-α, tumor necrosis factor-α.

D-GalN only-treated cells (Fig. 3C and D). These results indicated that hPH protected against D-GalN-induced hepatotoxicity in HepG2 cells. Changes in cellular morphology and cell viability were also evaluated to examine the protective effects of hPH in D-GalN-stimulated HepG2 cells. As shown in Fig. 3E, the D-GalN-stimulated HepG2 cells exhibited a marked reduction in the number of hepatocytes. However, hPH pretreatment effectively improved the D-GalN-mediated cell damages.

To examine the inhibitory mechanisms of hPH in D-GalN-induced cytotoxicity, the HepG2 cells were assessed by Annexin V and PI staining, followed by microplate analysis (Fig. 3F and G) or fluorescence microscopy (Fig. 3H). D-GalN stimulation alone facilitated the induction of apoptosis, including levels of Annexin V+ (841%)/PI+ (948%), compared with the

controls. By contrast, pretreatment with hPH significantly inhibited D-GalN-induced apoptosis (Annexin V+, 801%; PI+, 280%). D-GalN-induced DNA fragmentation was also effectively attenuated by hPH pretreatment (Fig. 3H). The present study further examined whether hPH regulated PARP-dependent cell death. D-GalN induced an increase of Bax (pro-apoptotic protein) and a decrease of Bcl-2 (anti-apoptotic protein) (Fig. 3I and J). Furthermore, the cleavage of PARP was inhibited in the HepG2 cells by pretreatment with hPH (Fig. 3I and J). These findings suggested that hPH treatment significantly improved hepatocyte degeneration through the attenuation of apoptosis in HepG2 cells.

hPH regulates D-GalN-mediated intracellular ROS generation and mitochondrial dysfunction. The rapid generation of
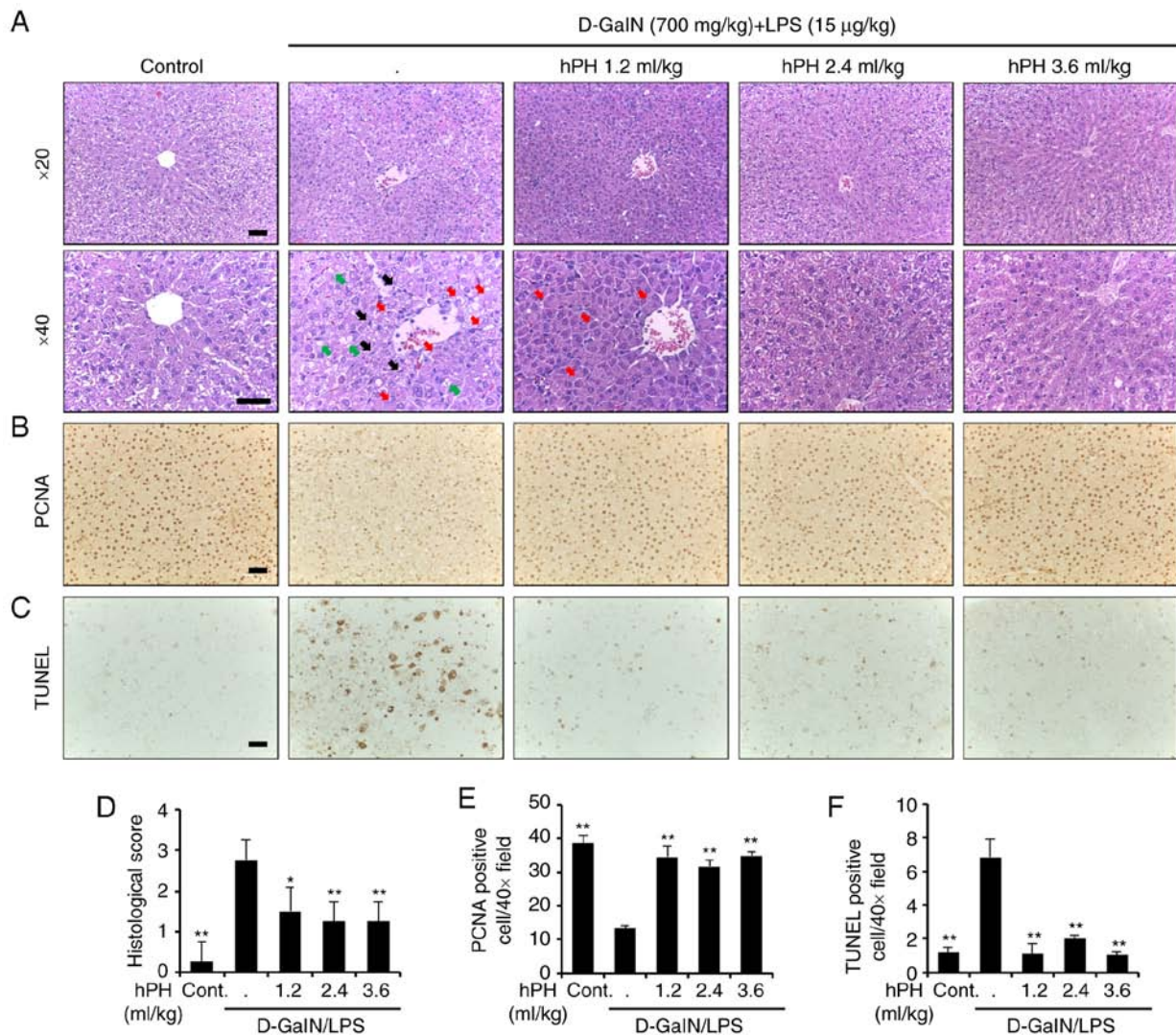
Figure 2. Effects of hPH treatment on D-GalN/LPS-induced acute liver failure in tissue degeneration and apoptosis. (A) Histopathological staining. Upper panel (magnification, x20), lower panel (magnification, x40). Scale bar=100 μm. The arrows indicate apoptotic hepatocytes (black), a severely affected region of a lobule containing ballooned hepatocytes (red), and hepatocytes expanded by fat vacuoles (green). (B) Images showing PCNA staining. Scale bar=100 μm. (C) Apoptotic response to D-GalN/LPS in the liver tissue of rats was investigated using TUNEL staining. Scale bar=100 μm. (D) Stained sections were graded for histopathology using a four-point scale (0-3), with 0, 1, 2, and 3 representing no damage, mild damage, moderate damage, and severe damage, respectively. (E) PCNA-positive cells were significantly less numerous in the D-GalN/LPS-treated group than in the control group; the addition of hPH led to significant overexpression of PCNA in the liver compared with D-GalN/LPS treatment alone. (F) TUNEL-positive cells was higher in number in the group treated with D-GalN/LPS alone compared with the control group. However, apoptotic induction by D-GalN/LPS was further reduced in the groups treated with 1.2, 2.4, and 3.6 ml/kg of hPH. All data are presented as the mean ± standard error of the mean. *P<0.05 and **P<0.01, vs. D-GalN/LPS group. hPH, human placental hydrolysate; D-GalN, D-galactosamine; LPS, lipopolysaccharide; PCNA, proliferating cell nuclear antigen; Cont, control.

ROS is associated with hyperpolarization of the mitochondrial membrane potential and apoptosis in D-GalN-treated hepatocytes (36). In addition, D-GalN-dependent cell necrosis is associated with mitochondrial membrane depolarization (37). To investigate whether the D-GalN-mediated increase in abnormal mitochondria was rescued by hPH treatment, the present study first evaluated mitochondrial morphology using Tomm20 (mitochondrial outer membrane) staining (Fig. 4A). Mitochondrial morphology was altered at 24 h in the D-GalN-stimulated HepG2 cells. However, the increased mitochondrial damage was attenuated significantly by hPH. In addition, mitochondrial mass decreased, by ~55%, in the D-GalN-stimulated HepG2 cells, and this was rescued by hPH pretreatment (Fig. 4B). ΔΨm was then evaluated using microplate analysis. The D-GalN-stimulated HepG2 cells

exhibited decreased ΔΨm; however, this decrease was significantly attenuated in the hPH-pretreated cells and unstimulated cells (Fig. 4C). These findings suggested that hPH improved D-GalN-mediated mitochondrial dysfunction by improving ΔΨm and inhibiting quantitative mitochondria loss.

Subsequently, the present study determined whether hPH was involved in the negative regulation of oxidative stress. The HepG2 cells were stimulated with D-GalN in the presence or absence of hPH, and ROS generation was determined using DCFH-DA or MitoSOX (mitochondrial-specific superoxide indicator) (38) as a probe for microplate analyses (Fig. 4D and E). D-GalN alone led to the potent intracellular generation of ROS, whereas the D-GalN-induced generation of ROS in HepG2 cells was attenuated significantly by hPH pretreatment (Fig. 4D). Mitochondrial ROS increased
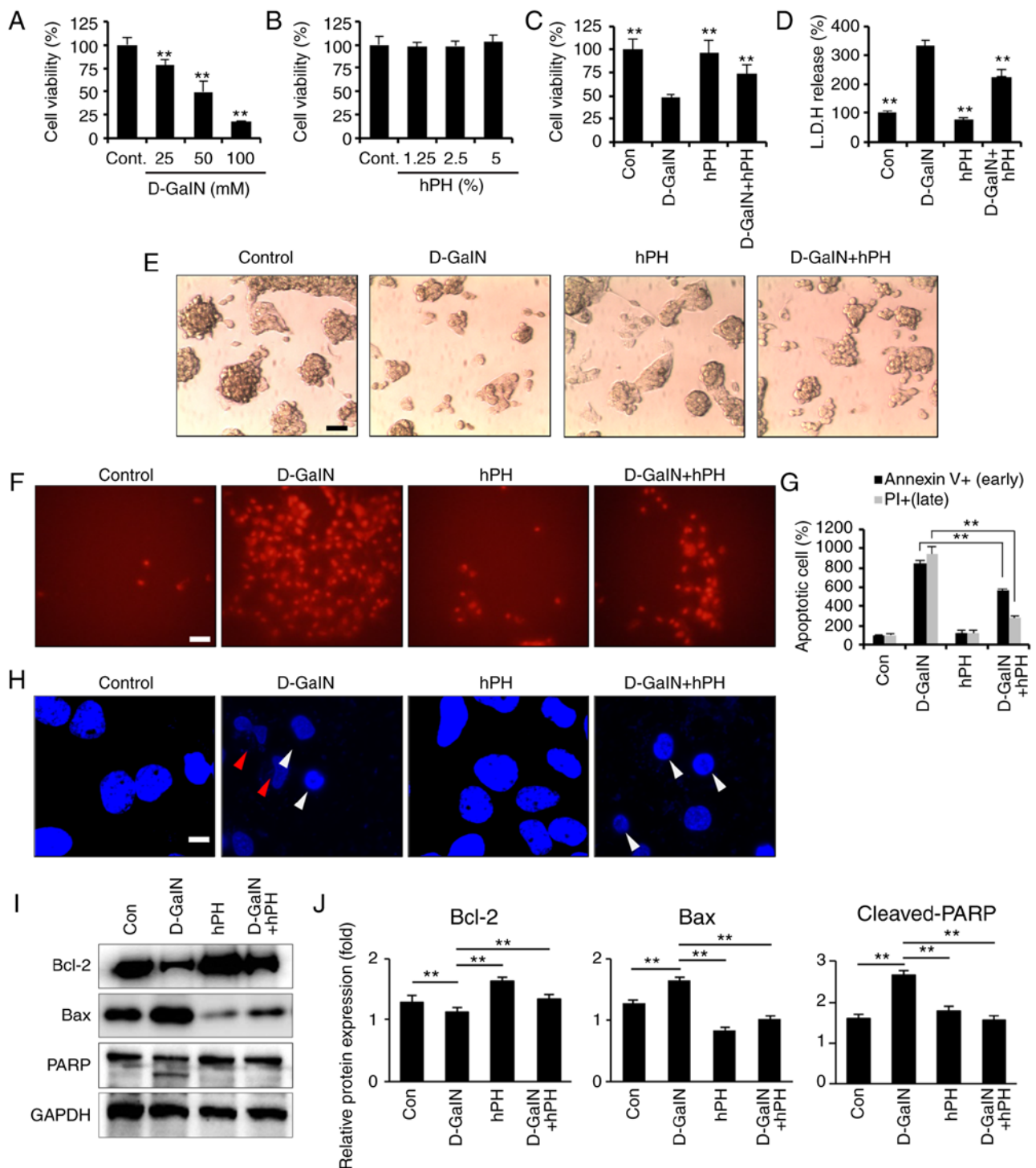
Figure 3. Effects of hPH treatment on D-GalN-induced apoptosis in HepG2 cells. (A) HepG2 cells were treated with 25, 50, or 100 mM D-GalN for 24 h. Treatment with 50 mM D-GalN yielded a cell viability of almost 50% compared with the vehicle control. The concentration of 50 mM D-GalN was used to determine the 50% inhibitory concentration. (B) HepG2 cells were treated with increasing concentrations of hPH or vehicle control for 24 h. HepG2 cells were treated with hPH (5%) for 2 h prior to D-GalN stimulation (50 mM). After 24 h, the hepatoprotective effects of hPH were assessed with the (C) Cell Counting Kit-8 assay and (D) LDH release test for cell viability, and with an (E) inverted phase-contrast microscope for morphological changes (scale bar=50 μm). HepG2 cells were stimulated with D-GalN (50 mM, 24 h) in the presence or absence of 5% hPH. (F) Cells were subjected to fluorescence microscopy (PI stain only) and (G) Annexin V/PI staining analyzed by a microplate (scale bar=50 μm). (H) DNA fragmentation (red arrow) and nuclear condensation (white arrow) were detected by DAPI staining under each condition (scale bar=5 μm). For western blot analysis, cell lysates were collected and subjected to sodium dodecyl sulfate-PAGE, followed by immunoblot analysis using anti-BCL2, anti-BAX and anti-PARP antibodies. Anti-GAPDH was used as a loading control. (I) Representative images and (J) densitometry. All data are presented as the mean ± standard error of the mean. **P<0.01, vs. D-GalN group. hPH, human placental hydrolysate; D-GalN, D-galactosamine; Cont, control; LDH, lactate dehydrogenase; BCL2, B-cell lymphoma 2; BAX, Bcl-2-associated X protein; PARP, poly (ADP) ribose polymerase; PI, propidium iodide.

significantly following treatment with D-GalN (Fig. 4E), whereas D-GalN-induced mitochondrial ROS generation was decreased by pretreatment with hPH. These results suggested that hPH protected against D-GalN-mediated
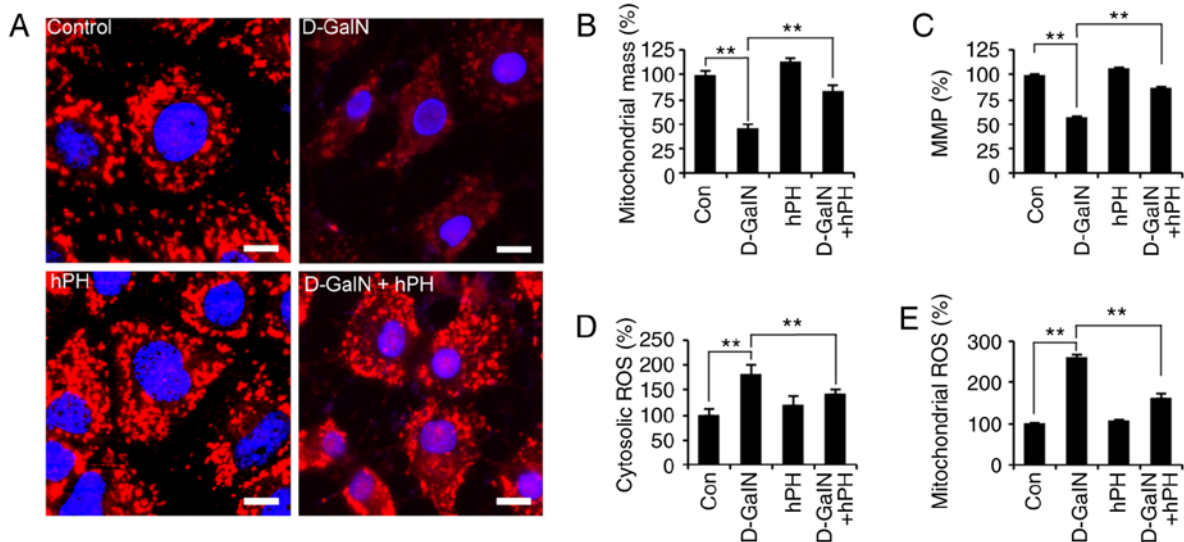
Figure 4. D-GalN-induced mitochondrial dysfunction and ROS overgeneration in HepG2 cells are improved by hPH treatment. HepG2 cells were stimulated with D-GalN (50 mM, 24 h) in the presence or absence of 5% hPH. (A) HepG2 cells post-hPH treatment were immunostained with anti-Tomm20 antibody, followed by the addition of Cy3-conjugated secondary antibody. Nuclei were identified using DAPI staining (scale bar=5 µm). (B) MitoTracker fluorescence signals for mitochondrial mass were measured. (C) ΔΨm was measured under the indicated conditions using the ΔΨm-sensitive fluorochrome MitoTracker Red CMXRos. (D) Cells were stained with 2',7'-dichlorofluorescin diacetate for 30 min to measure intracellular hydrogen peroxide. (E) Cells were stained with MitoSOX for 30 min to measure mitochondrial ROS. Bar graphs show relative analysis. All data are presented as the mean ± standard error of the mean. [**]P<0.01, vs. D-GalN group. hPH, human placental hydrolysate; D-GalN, D-galactosamine; Con, control; MMP/ΔΨm, mitochondrial membrane potential; ROS, reactive oxygen species.

apoptotic cell death by regulating the generation of cytosolic and mitochondrial ROS.

hPH regulates expression of antioxidant enzymes in HepG2 cells. As the induction of antioxidant enzymes is a universal stress response against liver degeneration and has been widely shown to have an anti-apoptotic effect, the expression levels of antioxidative enzymes SOD1, SOD2, GPx, and catalase were detected by western blot analysis (Fig. 5A). hPH induced antioxidative enzyme expression in the HepG2 cells. These enzymes were elevated 1 h following hPH treatment and were maintained at this level until 8 h. Furthermore, to investigate the antioxidant mechanisms of hPH, Nrf2 pathway-related gene expression on HepG2 cells was evaluated (Fig. 5B-D). The induction of Nrf2 upregulates antioxidant proteins, including SOD, catalase, and HO-1, reducing ROS (15). hPH treatment resulted in a significant decrease of Keap1 at 4-8 h. However, hPH increased the protein levels of cytoplasmic p-p62 and HO-1. Additionally, p62 was upregulated 4-8 h following hpH treatment (Fig. 5B). Furthermore, the expression of Nrf2 was decreased in the cytosol and increased in the nucleus (active Nrf2) following hPH treatment, indicating that translocation to the nucleus was affected by hPH treatment (Fig. 5C and D). Together, these findings indicated that the induction of antioxidative enzymes by hPH treatment was modulated by the Keap1-p62-Nrf2 pathway.

hPH minimizes the expression of damage-related molecules via the regulation of autophagy. Autophagy, mitochondria, and oxidative stress are closely intertwined in redox signalling (39). Additionally, D-GalN-induced cell damage regulates the autophagy process in early stages. To investigate whether the regulation of autophagy is influenced

by D-GalN stimulation and the effects of hPH, the present study measured the level of autophagy regulation by staining cells with anti-LC3 I/II antibody (Fig. 6A). LC3 I/II is an established autophagy marker due to its involvement in autophagosome membrane formation (40). In the present study, compared with the cells treated with vehicle control or D-GalN alone, the cells treated with hPH exhibited significantly fewer LC3 puncta per cell (Fig. 6A). The changes in autophagy-related genes were then quantified through assessment of RNA and protein levels in the hPH-treated HepG2 cells. As shown in Fig. 6B and C, hPH treatment induced a decrease in the conversion of LC3-I to LC3-II (lipidated form), the latter of which is a reliable marker of autophagosome generation. Furthermore, the expression levels of DRAM, CHOP, and p53 (proteins associated with autophagic cell death) indicated that a minimized autophagy process was induced in the hPH-treated cells (Fig. 6B) (20,41,42). Similarly, the transcription levels of autophagy-related genes (ATG8, CTSD, BECN1, and LAMP1) and of ER stress-related genes (ATF4, ATF6, and CHOP) were lower in the hPH-treated cells compared with those in cells treated with D-GalN only (Fig. 6C). These results suggested that hPH treatment minimized the escalation of D-GalN-induced autophagy processes in HepG2 cells.

Discussion

Apoptosis and oxidative stress are interrelated biological events that are involved in the pathogenesis of various diseases, including ALF (43-46). Emerging evidence suggests that D-GalN/LPS-induced oxidative stress gives rise to hepatic injuries resulting from oxidative stress and apoptosis, which parallel those of liver degeneration (6,7).
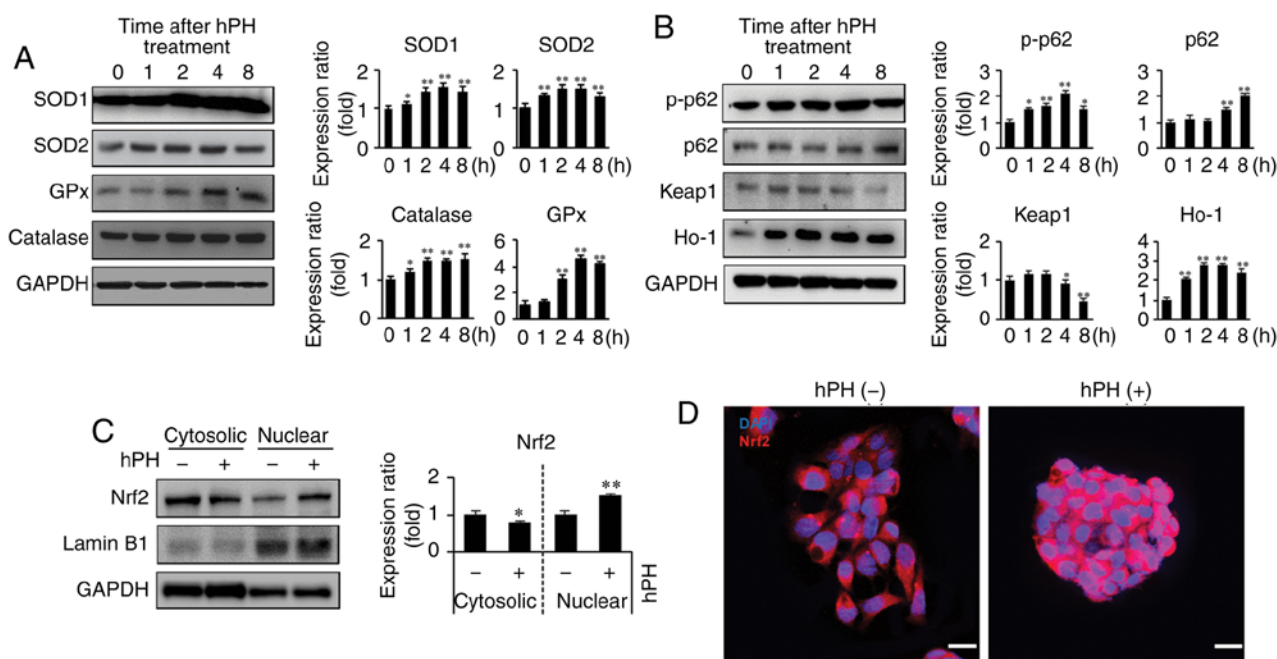
Figure 5. Upregulation of antioxidant enzymes and regulation of Keap1-Nrf2 in hPH-treated HepG2 cells. (A) Lysates from hPH-induced HepG2 cells were immunoblotted with anti-SOD-1, anti-SOD-2, anti-GPx, or anti-catalase antibodies. Representative images (left penal), densitometry results (right panel). All data are presented as the mean ± standard error of the mean. *P<0.05, **P<0.01 vs. 0 h time point. (B) Following treatment with hPH, the expression levels of p-p62, p62, Keap1, and HO-1 were determined by western blot analysis. Representative images (left penal), densitometry results (right panel). All data are presented as the mean ± standard error of the mean. *P<0.05, **P<0.01, vs. 0 h time point. (C) Nuclear localization of Nrf2 in hPH-treated HepG2 cells compared with untreated HepG2 cells. Lysates from hPH-treated HepG2 cells were immunoblotted with anti-Nrf2, anti-Lamin B1, or anti-GAPDH antibodies. Representative images (left penal), densitometry results (right panel). All data are presented as the mean ± standard error of the mean. *P<0.05, **P<0.01, vs. 0 h time point. (D) HepG2 cells post-hPH treatment were immunostained with anti-Nrf2 antibody. Nuclei were identified using DAPI staining (scale bar=20 μm). hPH, human placental hydrolysate; SOD, superoxide dismutase; GPx, glutathione peroxidase; Keap1, Kelch-like ECH2-associated protein 1; HO-1, heme oxygenase-1; p-p62; Nrf2, nuclear factor-E2-related factor 2.

In addition, D-GalN/LPS-induced ALF is widely accepted as an experimental liver injury animal model, contributing to investigation of the mechanisms underlying clinical liver injury and the development of efficient hepatoprotective materials (47-51). Accordingly, any approach that relieves apoptosis and oxidative stress *in vitro* and *in vivo* contributes to the prevention or treatment of ALF. In the present study, it was demonstrated that pretreatment with hPH attenuated acute liver injury associated with elevated serum levels of ALP, AST, LDH, and pro-inflammatory cytokines (IL-6 and TNF-α). Furthermore, it was found that apoptosis was increased following D-GalN/LPS injection, whereas pretreatment with hPH effectively inhibited tissue degeneration and increased cell death in D-GalN/LPS-induced acute liver injury. Pretreatment with hPH also reversed the extensive vacuolization, severe intrahepatic hemorrhage, destruction of nuclei, and loss of hepatic cords. Consistently, it has been reported that hPH possesses a variety of biological activities, including anti-inflammatory (26,52-56) and antioxidant (26,57-59) properties. Exposure to hazardous components from the environment can lead to pregnancy loss, uterine dysfunction, or fetal death (60). It has been reported that oxidative stress is mainly or partly involved in damage from these harmful environments (61). Therefore, the human placenta contains antioxidant defense substances to protect embryos from oxidative stress (62-64). Human placenta extract prepared from the placenta of healthy pregnant females is known to have various physiological actions,

including antioxidative properties (57,65). In the present study, hPH was prepared with human placenta, including umbilical cord, following the provision of consent from the pregnant women. The hydrolysate of human placenta is manufactured by a chemical process with HCl and pepsin, followed by dialysis, heat treatment and hydrolysis. This hydrolysate contains various amino acids, including arginine (0.08%), lysine (0.1%), phenylalanine (0.08%), tyrosine (0.03%), leucine (0.12%), methionine (0.03%), valine (0.04%), alanine (0.08%), serine (0.07%), and threonine (0.06%). Based on this, hPH is considered to contain the cleaved proteins of the amino acids and their active ingredients.

In previous studies, it has been reported that D-GalN leads to cytotoxicity and apoptotic cell death in HepG2 cells (66-68). D-GalN/LPS intoxication causes an imbalance between pro-oxidants and antioxidants, involving the excessive production of ROS and a deficiency of cellular antioxidants, including glutathione, catalase and SOD. Oxidative stress caused by D-GalN/LPS is a recognized phenomenon in liver damage (47,69-71). In addition, D-GalN/LPS induces loss of ΔΨm and production of ROS, resulting in liver damage (36,72-74). Mitochondria are the major subcellular organelles responsible for ROS production (75). The results of the present study demonstrated that hPH enhanced the expression of SOD-1, SOD-2, catalase and GPx, and increased the nuclear translocation of the Nrf2 via a Keap1-p62-Nrf2 mechanism. The upregulation of various important antioxidants is caused by the binding of Nrf2 to the ARE of
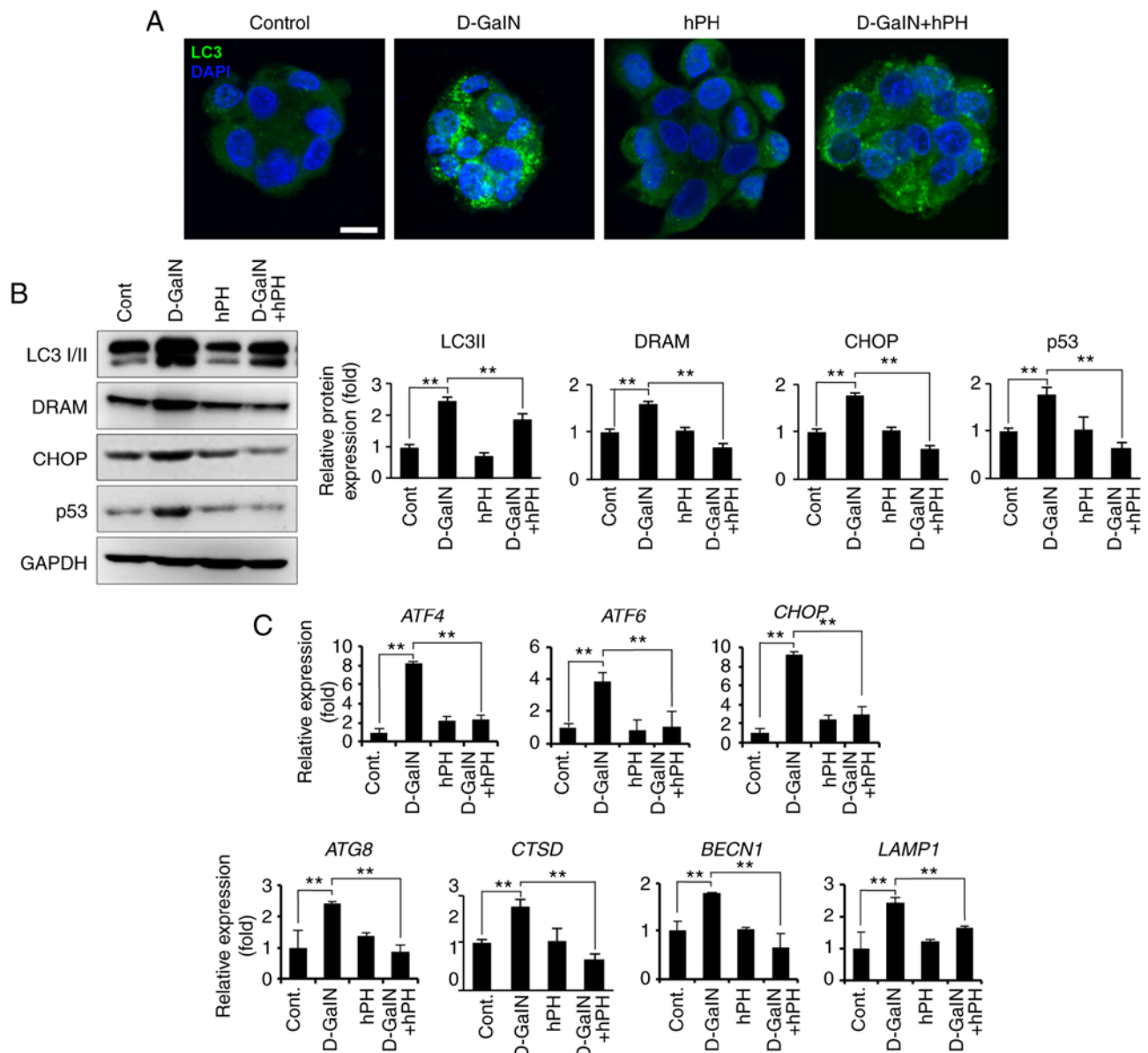
Figure 6. hPH treatment results in altered autophagy regulation in HepG2 cells following D-GalN stimulation. (A) HepG2 cells treated with hPH exhibit minimized autophagy flux. To detect autophagosomes, cells were immunostained with anti-LC3 antibody. Nuclei were identified using DAPI staining (scale bar=10 μm). (B) Cell lysates were immunoblotted with anti-LC3 I/II, anti-DRAM, anti-CHOP, anti-p53, or anti-GAPDH antibodies. Representative western blot images (left panel) and densitometry results (right panel). All data are presented as the mean ± standard error of the mean. **P<0.01, vs. D-GalN group. (C) Transcript levels of ER stress- and autophagy-related genes were determined by reverse transcription-quantitative polymerase chain reaction analysis. All data are presented as the mean ± standard error of the mean. **P<0.01, vs. D-GalN group. hPH, human placental hydrolysate; D-GalN, D-galactosamine; Cont, control; LC3, microtubule-associated protein 1A/1B-light chain 3; DRAM, damage-regulated autophagy modulator; CHOP, C/EBP homologous protein; ATF, activating transcription factor; BECN1; beclin 1; LAMP1, lysosomal-associated membrane protein 1.

antioxidant target proteins, including SOD, catalase, NQO1, GCLM and HO-1 (15,16). Nrf2 has been regarded as a novel therapeutic target for the treatment of liver disease (76-80). In Nrf2-deficient mice, the expression of various cytoprotective enzymes was decreased in hepatocytes, resulting in oxidative stress and markedly delayed liver regeneration (81). In addition, genetic disruption of Nrf2 triggers the progression of necroinflammation and hepatic fibrosis in Hfe$^{-/-}$ mice presenting with no liver injury (82). Pretreatment with sulforaphane prevents hepatic damage induced by intestinal ischemia/reperfusion in rats through an antioxidative effect via the Nrf2-ARE pathway (79). Another study showed that the expression of Nrf2 was upregulated to protect the liver

from inflammatory damage caused by oxidative stress during the development of non-alcoholic fatty liver and steatohepatitis (78). Additionally, Farombi et al reported that curcumin (diferuloymethane) administration promoted the nuclear translocation and ARE-binding of Nrf2, leading to prevention of dimethylnitrosamine-induced hepatotoxicity (76). In addition, β-cryptoxanthin was found to ameliorate visceral fat and cardiometabolic health risk factors by modulating the expression of nuclear factor-κB and Nrf2 in rats fed a high-fat diet (83).

Autophagy is an evolutionarily conserved homeostatic process and lysosome-dependent proteolytic pathway, which is involved in a variety of physiological and pathological

processes (84,85). According to previous data, autophagy is involved in major liver diseases, including liver ischemia/reperfusion injury, hepatitis B and C, hepatocellular carcinoma, alcoholic liver disease and non-alcoholic fatty liver disease (86). In addition, autophagy is induced to maintain healthy cells in the presence of TNF-, acetaminophen-, or ethanol-induced liver injury (87-89). However, excessive autophagy can cause autophagic cell death. Previously, autophagy has been shown to be elevated in concanavalin A-induced acute hepatitis, leading to the autophagic cell death of hepatoma cells in SCID/NOD mice (90). Furthermore, autophagy inhibition significantly improved liver graft dysfunction and the survival rate of recipient rats with 'cold ischemia-warm reperfusion injury' associated with liver transplantation (91), suggesting that autophagy can aggravate liver damage. In the present study, it was found that excessive autophagy was induced following D-GalN administration, and that pretreatment with hPH effectively suppressed this enhanced autophagy in D-GalN-induced HepG2 cells. It also indicated a regulatory pathway mechanism of autophagy induction and inhibition by D-GalN/hPH via the p53-DRAM-autophagy axis. The identification of DRAM as a p53 target mediating the induction of autophagy allowed for investigation of the role of autophagy in apoptosis (42). Liu *et al* reported that p53-induced apoptosis is primarily dependent on DRAM- and BAX-mediated autophagy in hepatosteatosis in oleic acid-treated HepG2 cells and high-fat diet mice (92). The induction of autophagy by the nuclear translocation of p53 involves the upregulation of DRAM and sestrin2 in p53-sufficient, but not in p53-deficient cells (93). The expression of CHOP is regulated transcriptionally and post-transcriptionally in hPH-induced HepG2 cells. CHOP, a multifunctional transcription factor in the ER stress response, promotes autophagic apoptosis induced by various stimuli, including tetrahydrocannabinol, 2-deoxy-D-glucose, rabbit hemorrhagic disease virus, and apoptosis-stimulating protein of p53-2 (94-97). The data obtained in the present study also demonstrated that hPH led to downregulation of the ER stress-related downstream targets, ATF4 and ATF6, in D-GalN-treated HepG2 cells. Based on the above findings, it was concluded that autophagy, apoptosis and ER stress are closely associated with each other, supported by the results of the present study. D-GalN stimulation increased the expression levels of DRAM, CHOP and the apoptosis-related protein p53 in HepG2 cells, whereas hPH pretreatment reversed the expression of these proteins. hPH pretreatment also resulted in LC3 lipidation, but meaningfully minimized autophagosome expression compared with D-GalN alone.

In previous animal studies, early onset autophagy has been shown to increase liver injury, however, this observation has not been corroborated in patient populations. Therefore, the epidemiological relevance of autophagy and liver damage require investigation in the future. Taken together, the results of the present study showed that hPH had a protective effect on hepatocyte apoptosis through antioxidative modulation and minimization of the autophagy process, which resulted in the inhibition of hepatocytotoxicity. This may be useful as a target for the treatment of acute liver injury. The identification of this pathway can assist in understanding the molecular events leading to the activation of oxidative stress- and autophagy-mediated cell death in human disease, and contribute to the design of novel therapeutic strategies for inhibiting liver disease and preventing fulminant hepatic failure.

Availability of data and materials

The analyzed data sets generated during the study are available from the corresponding author on reasonable request.

Authors' contributions

BJK, THK, DHB, JN, and MJC designed experiments; DHB, JN, and MJC performed experiments; MJK, BCL, THK, DHB, JN, MJC, CTO, JYK, and HJH analyzed data; CTO, JYK, and HJH prepared materials; DHB, JN, and MJC prepared figures; BJK, THK, DHB, and JN wrote the manuscript. BJK and THK had primary responsibility for final content. All authors have read and approved the final manuscript.

Ethics approval and consent to participate

The present study was approved by the Institutional Animal Care and Use Committee of Chung-Ang University (2017-00003). Placental tissues were used following the provision of informed consent from the pregnant women.

Patient consent for publication

Not applicable.

Competing interests

The authors declare that they have no competing interests.

References

1. Bernal W, Auzinger G, Dhawan A and Wendon J: Acute liver failure. Lancet 376: 190-201, 2010.
2. Han DW: Intestinal endotoxemia as a pathogenetic mechanism in liver failure. World J Gastroenterol 8: 961-965, 2002.
3. Sathivel A, Balavinayagamani, Hanumantha Rao BR and Devaki T: Sulfated polysaccharide isolated from Ulva lactuca attenuates d-galactosamine induced DNA fragmentation and necrosis during liver damage in rats. Pharm Biol 52: 498-505, 2014.
4. Masaki T, Chiba S, Tatsukawa H, Yasuda T, Noguchi H, Seike M and Yoshimatsu H: Adiponectin protects LPS-induced liver injury through modulation of TNF-α in KK-Ay obese mice. Hepatology 40: 177-184, 2004.
5. Wu Z, Han M, Chen T, Yan W and Ning Q: Acute liver failure: Mechanisms of immune-mediated liver injury. Liver Int 30: 782-794, 2010.

6. Sheriff SA, Shaik Ibrahim S, Devaki T, Chakraborty S, Agarwal S and Pérez-Sánchez H: Lycopene prevents mitochondrial dysfunction during d-galactosamine/lipopolysaccharide-induced fulminant hepatic failure in albino rats. J Proteome Res 16: 3190-3199, 2017.

7. Dong L, Yin L, Quan H, Chu Y and Lu J: Hepatoprotective effects of kaempferol-3-O-α-l-arabinopyranosyl-7-O-α-l-rhamn opyranoside on d-Galactosamine and lipopolysaccharide caused hepatic failure in mice. Molecules 22: E1755, 2017.

8. Lee SB, Kang JW, Kim SJ, Ahn J, Kim J and Lee SM: Afzelin ameliorates D-galactosamine and lipopolysaccharide-induced fulminant hepatic failure by modulating mitochondrial quality control and dynamics. Br J Pharmacol 174: 195-209, 2017.

9. Decker CW, Casian JG, Nguyen KT, Horton LA, Rao MP, Silkwood KH and Han D: The critical role of mitochondria in drug-induced liver injury. In: Molecules, Systems and Signaling in Liver Injury. Springer, pp159-181, 2017.

10. Nguyen T, Nioi P and Pickett CB: The Nrf2-antioxidant response element signaling pathway and its activation by oxidative stress. J Biol Chem 284: 13291-13295, 2009.

11. Bryan HK, Olayanju A, Goldring CE and Park BK: The Nrf2 cell defence pathway: Keap1-dependent and -independent mechanisms of regulation. Biochem Pharmacol 85: 705-717, 2013.

12. Zhou R, Lin J and Wu D: Sulforaphane induces Nrf2 and protects against CYP2E1-dependent binge alcohol-induced liver steatosis. Biochim Biophys Acta 1840: 209-218, 2014.

13. Jiang T, Huang Z, Lin Y, Zhang Z, Fang D and Zhang DD: The protective role of Nrf2 in streptozotocin-induced diabetic nephropathy. Diabetes 59: 850-860, 2010.

14. Kobayashi A, Kang MI, Okawa H, Ohtsuji M, Zenke Y, Chiba T, Igarashi K and Yamamoto M: Oxidative stress sensor Keap1 functions as an adaptor for Cul3-based E3 ligase to regulate proteasomal degradation of Nrf2. Mol Cell Biol 24: 7130-7139, 2004.

15. Bataille A and Manautou J: Nrf2: A potential target for new therapeutics in liver disease. Clin Pharmacol Ther 92: 340-348, 2012.

16. Jian Z, Li K, Song P, Zhu G, Zhu L, Cui T, Liu B, Tang L, Wang X, Wang G, et al: Impaired activation of the Nrf2-ARE signaling pathway undermines H_2O_2-induced oxidative stress response: A possible mechanism for melanocyte degeneration in vitiligo. J Invest Dermatol 134: 2221-2230, 2014.

17. Mizushima N, Levine B, Cuervo AM and Klionsky DJ: Autophagy fights disease through cellular self-digestion. Nature 451: 1069-1075, 2008.

18. Mizushima N and Komatsu M: Autophagy: Renovation of cells and tissues. Cell 147: 728-741, 2011.

19. Gozuacik D and Kimchi A: Autophagy and cell death. Curr Top Dev Biol 78: 217-245, 2007.

20. Crighton D, Wilkinson S, O'Prey J, Syed N, Smith P, Harrison PR, Gasco M, Garrone O, Crook T and Ryan KM: DRAM, a p53-induced modulator of autophagy, is critical for apoptosis. Cell 126: 121-134, 2006.

21. Tonello G, Daglio M, Zaccarelli N, Sottofattori E, Mazzei M and Balbi A: Characterization and quantitation of the active polynucleotide fraction (PDRN) from human placenta, a tissue repair stimulating agent. J Pharm Biomed Anal 14: 1555-1560, 1996.

22. Sur TK, Biswas TK, Ali L and Mukherjee B: Anti-inflammatory and anti-platelet aggregation activity of human placental extract. Acta Pharmacol Sin 24: 187-192, 2003.

23. Chakraborty PD and Bhattacharyya D: Isolation of fibronectin type III like peptide from human placental extract used as wound healer. J Chromatogr B Analyt Technol Biomed Life Sci 818: 67-73, 2005.

24. Choi JY, Lee K, Lee SM, Yoo SH, Hwang SG, Choi JY, Lee SW, Hwang JS, Kim KK, Kang HC, et al: Efficacy and safety of human placental extract for alcoholic and nonalcoholic steatohepatitis: An open-label, randomized, comparative study. Biol Pharm Bull 37: 1853-1859, 2014.

25. Shimokobe H, Sumida Y, Tanaka S, Mori K, Kitamura Y, Fukumoto K, Kakutani A, Ohno T, Kanemasa K, Imai S, et al: Human placental extract treatment for non-alcoholic steatohepatitis non-responsive to lifestyle intervention: A pilot study. Hepatol Res 45: 1034-1040, 2015.

26. Park S, Phark S, Lee M, Lim J and Sul D: Anti-oxidative and anti-inflammatory activities of placental extracts in benzo[a] pyrene-exposed rats. Placenta 31: 873-879, 2010.

27. Camargo CA Jr, Madden JF, Gao W, Selvan RS and Clavien P: Interleukin-6 protects liver against warm ischemia/reperfusion injury and promotes hepatocyte proliferation in the rodent. Hepatology 26: 1513-1520, 1997.

28. Okoh VO, Felty Q, Parkash J, Poppiti R and Roy D: Reactive oxygen species via redox signaling to PI3K/AKT pathway contribute to the malignant growth of 4-hydroxy estradiol-transformed mammary epithelial cells. PLoS One 8: e54206, 2013.

29. Jasek E, Lis GJ, Jasińska M, Jurkowska H and Litwin JA: Effect of histone deacetylase inhibitors trichostatin A and valproic acid on etoposide-induced apoptosis in leukemia cells. Anticancer Res 32: 2791-2799, 2012.

30. Livak KJ and Schmittgen TD: Analysis of relative gene expression data using real-time quantitative PCR and the 2(-Delta Delta C(T)) method. Methods 25: 402-408, 2001.

31. Cassidy W and Reynolds T: Serum lactic dehydrogenase in the differential diagnosis of acute hepatocellular injury. J Clin Gastroenterol 19: 118-121, 1994.

32. Rolando N, Wade J, Davalos M, Wendon J, Philpott-Howard J and Williams R: The systemic inflammatory response syndrome in acute liver failure. Hepatology 32: 734-739, 2000.

33. Guicciardi M and Gores GJ: Apoptosis: A mechanism of acute and chronic liver injury. Gut 54: 1024-1033, 2005.

34. Stachlewitz RF, Seabra V, Bradford B, Bradham CA, Rusyn I, Germolec D and Thurman RG: Glycine and uridine prevent d-galactosamine hepatotoxicity in the rat: Role of kupffer cells. Hepatology 29: 737-745, 1999.

35. Thabrew MI, Hughes RD and McFarlane IG: Screening of hepatoprotective plant components using a HepG2 cell cytotoxicity assay. J Pharm Pharmacol 49: 1132-1135, 1997.

36. González R, Ferrín G, Hidalgo AB, Ranchal I, López-Cillero P, Santos-Gónzalez M, López-Lluch G, Briceño J, Gómez MA, Poyato A, et al: N-acetylcysteine, coenzyme Q10 and superoxide dismutase mimetic prevent mitochondrial cell dysfunction and cell death induced by d-galactosamine in primary culture of human hepatocytes. Chem Biol Interact 181: 95-106, 2009.

37. Zhao Y, Li S, Childs EE, Kuharsky DK and Yin XM: Activation of pro-death Bcl-2 family proteins and mitochondria apoptosis pathway in tumor necrosis factor-α-induced liver injury. J Biol Chem 276: 27432-27440, 2001.

38. Kuznetsov AV, Kehrer I, Kozlov AV, Haller M, Redl H, Hermann M, Grimm M and Troppmair J: Mitochondrial ROS production under cellular stress: Comparison of different detection methods. Anal Bioanal Chem 400: 2383-2390, 2011.

39. Lee J, Giordano S and Zhang J: Autophagy, mitochondria and oxidative stress: Cross-talk and redox signalling. Biochem J 441: 523-540, 2012.

40. Yang Z and Klionsky DJ: Mammalian autophagy: Core molecular machinery and signaling regulation. Curr Opin Cell Biol 22: 124-131, 2010.

41. Liu GY, Jiang XX, Zhu X, He WY, Kuang YL, Ren K, Lin Y and Gou X: ROS activates JNK-mediated autophagy to counteract apoptosis in mouse mesenchymal stem cells in vitro. Acta Pharmacol Sin 36: 1473-1479, 2015.

42. Maiuri MC, Zalckvar E, Kimchi A and Kroemer G: Self-eating and self-killing: Crosstalk between autophagy and apoptosis. Nat Rev Mol Cell Biol 8: 741-752, 2007.

43. Cichoż-Lach H and Michalak A: Oxidative stress as a crucial factor in liver diseases. World J Gastroenterol 20: 8082-8091, 2014.

44. Jenner P: Oxidative stress in Parkinson's disease. Ann Neurol 53 (Suppl 3): S26-S38, 2003.

45. Kujoth G, Hiona A, Pugh T, Someya S, Panzer K, Wohlgemuth SE, Hofer T, Seo AY, Sullivan R, Jobling WA, et al: Mitochondrial DNA mutations, oxidative stress, and apoptosis in mammalian aging. Science 309: 481-484, 2005.

46. Radi E, Formichi P, Battisti C and Federico A: Apoptosis and oxidative stress in neurodegenerative diseases. J Alzheimers Dis 42 (Suppl 3): S125-S152, 2014.

47. Osakabe N, Yasuda A, Natsume M, Sanbongi C, Kato Y, Osawa T and Yoshikawa T: Rosmarinic acid, a major polyphenolic component of Perilla frutescens, reduces lipopolysaccharide (LPS)-induced liver injury in D-galactosamine (D-GalN)-sensitized mice. Free Radic Biol Med 33: 798-806, 2002.

48. Nowak M, Gaines GC, Rosenberg J, Minter R, Bahjat FR, Rectenwald J, MacKay SL, Edwards CK III and Moldawer LL: LPS-induced liver injury in D-galactosamine-sensitized mice requires secreted TNF-alpha and the TNF-p55 receptor. Am J Physiol Regul Integr Comp Physiol 278: R1202-R1209, 2000.

49. Wu YL, Lian LH, Wan Y and Nan JX: Baicalein inhibits nuclear factor-κB and apoptosis via c-FLIP and MAPK in D-GalN/LPS induced acute liver failure in murine models. Chem Biol Interact 188: 526-534, 2010.

50. Chen L, Ren F, Zhang H, Wen T, Piao Z, Zhou L, Zheng S, Zhang J, Chen Y, Han Y, *et al*: Inhibition of glycogen synthase kinase 3β ameliorates D-GalN/LPS-induced liver injury by reducing endoplasmic reticulum stress-triggered apoptosis. PloS One 7: e45202, 2012.
51. Wang H, Xu DX, Lv JW, Ning H and Wei W: Melatonin attenuates lipopolysaccharide (LPS)-induced apoptotic liver damage in D-galactosamine-sensitized mice. Toxicology 237: 49-57, 2007.
52. Kawakatsu M, Urata Y, Goto S, Ono Y and Li TS: Placental extract protects bone marrow-derived stem/progenitor cells against radiation injury through anti-inflammatory activity. J Radiat Res 54: 268-276, 2012.
53. Park JY, Lee J, Jeong M, Min S, Kim SY, Lee H, Lim Y and Park HJ: Effect of Hominis Placenta on cutaneous wound healing in normal and diabetic mice. Nutri Res Pract 8: 404-409, 2014.
54. Lee KH, Kim TH, Lee WC, Kim SH, Lee SY and Lee SM: Anti-inflammatory and analgesic effects of human placenta extract. Nat Prod Res 25: 1090-1100, 2011.
55. Lee KW, Ji HM, Kim DW, Choi SM, Kim S and Yang EJ: Effects of Hominis placenta on LPS-induced cell toxicity in BV2 microglial cells. J Ethnopharmacol 147: 286-292, 2013.
56. Akagi H, Imamura Y, Makita Y, Nakamura H, Hasegawa N, Fujiwara SI and Wang PL: Evaluation of collagen type-1 production and anti-inflammatory activities of human placental extracts in human gingival fibroblasts. J Hard Tissue Biol 25: 277-281, 2016.
57. Watanabe S, Togashi S, Takahashi N and Fukui T: L-tryptophan as an antioxidant in human placenta extract. J Nutri Sci Vitaminol (Tokyo) 48: 36-39, 2002.
58. Togashi SI, Takahashi N, Iwama M, Watanabe S, Tamagawa K and Fukui T: Antioxidative collagen-derived peptides in human-placenta extract. Placenta 23: 497-502, 2002.
59. Rozanova S, Cherkashina Y, Repina S, Rozanova K and Nardid O: Protective effect of placenta extracts against nitrite-induced oxidative stress in human erythrocytes. Cell Mol Biol Lett 17: 240-248, 2012.
60. Halliwell B and Gutteridge JM: Free Radicals in Biology and Medicine. Oxford University Press, USA, 2015.
61. Wells PG and Winn LM: Biochemical toxicology of chemical teratogenesis. Crit Rev Biochem Mol Biol 31: 1-40, 1996.
62. Avissar N, Whitin JC, Allen PZ, Wagner DD, Liegey P and Cohen HJ: Plasma selenium-dependent glutathione peroxidase. Cell of origin and secretion. J Biol Chem 264: 15850-15855, 1989.
63. Thomas EL, Learn DB, Jefferson MM and Weatherred W: Superoxide-dependent oxidation of extracellular reducing agents by isolated neutrophils. J Biol Chem 263: 2178-2186, 1988.
64. Kankofer M: Antioxidative defence mechanisms against reactive oxygen species in bovine retained and not-retained placenta: Activity of glutathione peroxidase, glutathione transferase, catalase and superoxide dismutase. Placenta 22: 466-472, 2001.
65. Mochizuki H and Kada T: Restorative effects of human placenta extract in X-ray-irradiated mice. J Radiat Res 23: 403-410, 1982.
66. González R, Collado JA, Nell S, Briceño J, Tamayo MJ, Fraga E, Bernardos A, López-Cillero P, Pascussi JM, Rufián S, *et al*: Cytoprotective properties of α-tocopherol are related to gene regulation in cultured D-galactosamine-treated human hepatocytes. Free Radic Biol Med 43: 1439-1452, 2007.
67. Siendones E, Fouad D, Abou-Elella AMKE, Quintero A, Barrera P and Muntané J: Role of nitric oxide in d-galactosamine-induced cell death and its protection by PGE 1 in cultured hepatocytes. Nitric Oxide 8: 133-143, 2003.
68. Mahmoud MF, Hamdan DI, Wink M and El-Shazly AM: Hepatoprotective effect of limonin, a natural limonoid from the seed of Citrus aurantium var. bigaradia, on D-galactosamine-induced liver injury in rats. Naunyn-Schmiedebergs Arch Pharmacol 387: 251-261, 2014.
69. Wang Y, Li Y, Xie J, Zhang Y, Wang J, Sun X and Zhang H: Protective effects of probiotic Lactobacillus casei Zhang against endotoxin-and d-galactosamine-induced liver injury in rats via anti-oxidative and anti-inflammatory capacities. Int Immunopharmacol 15: 30-37, 2013.
70. Xia X, Su C, Fu J, Zhang P, Jiang X, Xu D, Hu L, Song E and Song Y: Role of α-lipoic acid in LPS/d-GalN induced fulminant hepatic failure in mice: Studies on oxidative stress, inflammation and apoptosis. Int Immunopharmacol 22: 293-302, 2014.
71. Shin JW, Wang JH, Park HJ, Choi MK, Kim HG and Son CG: Herbal formula CGX ameliorates LPS/D-galactosamine-induced hepatitis. Food Chem Toxicol 49: 1329-1334, 2011.
72. Lee HJ, Oh YK, Rhee M, Lim JY, Hwang JY, Park YS, Kwon Y, Choi KH, Jo I, Park SI, *et al*: The role of STAT1/IRF-1 on synergistic ROS production and loss of mitochondrial transmembrane potential during hepatic cell death induced by LPS/d-GalN. J Mol Biol 369: 967-984, 2007.
73. Liu LM, Zhang JX, Luo J, Guo HX, Deng H, Chen JY and Sun SL: A role of cell apoptosis in lipopolysaccharide (LPS)-induced nonlethal liver injury in D-galactosamine (D-GalN)-sensitized rats. Dig Dis Sci 53: 1316-1324, 2008.
74. Soriano ME, Nicolosi L and Bernardi P: Desensitization of the permeability transition pore by cyclosporin A prevents activation of the mitochondrial apoptotic pathway and liver damage by tumor necrosis factor-alpha. J Biol Chem 279: 36803-36808, 2004.
75. Indo HP, Davidson M, Yen HC, Suenaga S, Tomita K, Nishii T, Higuchi M, Koga Y, Ozawa T and Majima HJ: Evidence of ROS generation by mitochondria in cells with impaired electron transport chain and mitochondrial DNA damage. Mitochondrion 7: 106-118, 2007.
76. Farombi EO, Shrotriya S, Na HK, Kim SH and Surh YJ: Curcumin attenuates dimethylnitrosamine-induced liver injury in rats through Nrf2-mediated induction of heme oxygenase-1. Food Chem Toxicol 46: 1279-1287, 2008.
77. Klaassen CD and Reisman SA: Nrf2 the rescue: Effects of the antioxidative/electrophilic response on the liver. Toxicol Appl Pharmacol 244: 57-65, 2010.
78. Xu W, Shao L, Zhou C, Wang H and Guo J: Upregulation of Nrf2 expression in non-alcoholic fatty liver and steatohepatitis. Hepatogastroenterology 58: 2077-2080, 2011.
79. Zhao HD, Zhang F, Shen G, Li YB, Li YH, Jing HR, Ma LF, Yao JH and Tian XF: Sulforaphane protects liver injury induced by intestinal ischemia reperfusion through Nrf2-ARE pathway. World J Gastroenterol 16: 3002-3010, 2010.
80. Pan CW, Pan ZZ, Hu JJ, Chen WL, Zhou GY, Lin W, Jin LX and Xu CL: Mangiferin alleviates lipopolysaccharide and D-galactosamine-induced acute liver injury by activating the Nrf2 pathway and inhibiting NLRP3 inflammasome activation. Eur J Pharmacol 770: 85-91, 2016.
81. Beyer TA, Xu W, Teupser D, auf dem Keller U, Bugnon P, Hildt E, Thiery J, Kan YW and Werner S: Impaired liver regeneration in Nrf2 knockout mice: Role of ROS-mediated insulin/IGF-1 resistance. EMBO J 27: 212-223, 2008.
82. Duarte TL, Caldas C, Santos AG, Silva-Gomes S, Santos-Gonçalves A, Martins MJ, Porto G and Lopes JM: Genetic disruption of NRF2 promotes the development of necroinflammation and liver fibrosis in a mouse model of HFE-hereditary hemochromatosis. Redox Biol 11: 157-169, 2017.
83. Sahin K, Orhan C, Akdemir F, Tuzcu M, Sahin N, Yılmaz I and Juturu V: β-Cryptoxanthin ameliorates metabolic risk factors by regulating NF-κB and Nrf2 pathways in insulin resistance induced by high-fat diet in rodents. Food Chem Toxicol 107: 270-279, 2017.
84. Choi AM, Ryter SW and Levine B: Autophagy in human health and disease. N Engl J Med 368: 651-662, 2013.
85. Uchiyama Y, Shibata M, Koike M, Yoshimura K and Sasaki M: Autophagy-physiology and pathophysiology. Histochem Cell Biol 129: 407-420, 2008.
86. Rautou PE, Mansouri A, Lebrec D, Durand F, Valla D and Moreau R: Autophagy in liver diseases. J Hepatol 53: 1123-1134, 2010.
87. Amir M, Zhao E, Fontana L, Rosenberg H, Tanaka K, Gao G and Czaja MJ: Inhibition of hepatocyte autophagy increases tumor necrosis factor-dependent liver injury by promoting caspase-8 activation. Cell Death Differ 20: 878-887, 2013.
88. Donohue TM Jr: Autophagy and ethanol-induced liver injury. World J Gastroenterol 15: 1178-1185, 2009.
89. Lin Z, Wu F, Lin S, Pan X, Jin L, Lu T, Shi L, Wang Y, Xu A and Li X: Adiponectin protects against acetaminophen-induced mitochondrial dysfunction and acute liver injury by promoting autophagy in mice. J Hepatol 61: 825-831, 2014.
90. Chang CP and Lei HY: Autophagy induction in T cell-independent acute hepatitis induced by concanavalin A in SCID/NOD mice. Int J Immunopathol Pharmacol 21: 817-826, 2008.
91. Gotoh K, Lu Z, Morita M, Shibata M, Koike M, Waguri S, Dono K, Doki Y, Kominami E, Sugioka A, *et al*: Participation of autophagy in the initiation of graft dysfunction after rat liver transplantation. Autophagy 5: 351-360, 2009.

92. Liu K, Lou J, Wen T, Yin J, Xu B, Ding W, Wang A, Liu D, Zhang C, Chen D and Li N: Depending on the stage of hepatosteatosis, p53 causes apoptosis primarily through either DRAM-induced autophagy or BAX. Liver Int 33: 1566-1574, 2013.
93. Maiuri MC, Malik SA, Morselli E, Kepp O, Criollo A, Mouchel PL, Carnuccio R and Kroemer G: Stimulation of autophagy by the p53 target gene Sestrin2. Cell Cycle 8: 1571-1576, 2009.
94. Salazar M, Carracedo A, Salanueva ÍJ, Hernández-Tiedra S, Lorente M, Egia A, Vázquez P, Blázquez C, Torres S, García S, et al: Cannabinoid action induces autophagy-mediated cell death through stimulation of ER stress in human glioma cells. J Clin Invest 119: 1359-1372, 2009.
95. Xi H, Kurtoglu M, Liu H, Wangpaichitr M, You M, Liu X, Savaraj N and Lampidis TJ: 2-Deoxy-D-glucose activates autophagy via endoplasmic reticulum stress rather than ATP depletion. Cancer Chemother Pharmacol 67: 899-910, 2011.
96. Liu K, Shi Y, Guo X, Wang S, Ouyang Y, Hao M, Liu D, Qiao L, Li N, Zheng J and Chen D: CHOP mediates ASPP2-induced autophagic apoptosis in hepatoma cells by releasing Beclin-1 from Bcl-2 and inducing nuclear translocation of Bcl-2. Cell Death Dis 5: e1323, 2014.
97. Tuñón MJ, San-Miguel B, Crespo I, Laliena A, Vallejo D, Álvarez M, Prieto J and González-Gallego J: Melatonin treatment reduces endoplasmic reticulum stress and modulates the unfolded protein response in rabbits with lethal fulminant hepatitis of viral origin. J Pineal Res 55: 221-228, 2013.